

A Gaussian smooth transition vector autoregressive model: An application to the macroeconomic effects of severe weather shocks

Markku Lanne Savi Virolainen
University of Helsinki

Abstract

We introduce a new smooth transition vector autoregressive model with a Gaussian conditional distribution and transition weights that, for a p th order model, depend on the full distribution of the preceding p observations. Specifically, the transition weight of each regime increases in its relative weighted likelihood. This data-driven approach facilitates capturing complex switching dynamics, enhancing the identification of gradual regime shifts. In an empirical application to the macroeconomic effects of a severe weather shock, we find that in monthly U.S. data from 1961:1 to 2022:3, the impacts of the shock are stronger in the regime prevailing in the early part of the sample and in certain crisis periods than in the regime dominating the latter part of the sample. This suggests overall adaptation of the U.S. economy to increased severe weather over time.

Keywords: smooth transition VAR, nonlinear SVAR, structural smooth transition vector autoregression, regime-switching

The authors thank Pentti Saikkonen for the useful discussions and the Research Council of Finland for financial support (Grant 347986).

Contact address: Savi Virolainen, Faculty of Social Sciences, University of Helsinki, P. O. Box 17, FI-00014 University of Helsinki, Finland; e-mail: savi.virolainen@helsinki.fi. ORCID ID: 0000-0002-5075-6821.
The authors have no conflict of interest to declare.

1 Introduction

Smooth transition vector autoregressive (STVAR) models have gained attention in the literature due to their ability to capture nonlinear dynamics in time series data (see, e.g., Hubrich and Teräsvirta, 2013, and the references therein). They provide a flexible framework for modelling autoregressive systems that exhibit gradual shifts in parameter values. Moreover, structural STVAR models allow to trace out the causal effects of economic shocks, which may be asymmetric with respect to the sign and size of the shock as well as to the initial state of the economy.

STVAR models extend the conventional vector autoregressive (VAR) models by allowing for smooth transitions between regimes, each of which is characterized by a linear vector autoregression with different autoregressive coefficients or error term covariance matrices. In this paper, we consider STVAR models in which, at each point of time, the observation is a weighted average of the conditional means of the regimes plus a random error whose covariance matrix is a weighted average of the covariance matrices of the regimes. Different STVAR models are obtained by specifying the transition weights or the error distribution in various ways. In our model, the weights are expressed in terms of time-varying transition weights that depend on the preceding observations.

In particular, we introduce a new STVAR model that we call the Gaussian smooth transition vector autoregressive (GSTVAR) model. It assumes a Gaussian conditional distribution and adopts transition weights that are similar to the mixing weights of the Gaussian mixture vector autoregressive (GMVAR) model of Kalliovirta, Meitz, and Saikkonen (2016). For a p th order model, the transition weights depend on the full distribution of the preceding p observations, thereby allowing to capture complicated switching dynamics. Specifically, the greater the relative weighted likelihood of a regime is, the greater its transition weight is, which facilitates associating statistical characteristics and economic interpretations to the

regimes. In contrast to the GMVAR model, which incorporates unobserved discrete regime-switches, our GSTVAR model allows for capturing gradual shifts in the dynamics of the data. The GSTVAR model also has the advantage in structural analysis that, unlike in the GMVAR model, identified structural shocks can be recovered from the fitted model.

A variety of alternative STVAR models have been proposed in the previous literature, each characterized by a different transition weight function. A popular choice is to specify logistic transition weights and employ a logistic STVAR (LSTVAR) model (Anderson and Vahid, 1998). Another common alternative is the threshold VAR (TVAR) model (Tsay, 1998), which features discrete regimes such that the regime switches when a switching variable passes some threshold value. The LSTVAR and TVAR models have clear interpretations of the regimes and can accommodate exogenous as well as endogenous switching variables. Therefore, they are well-suited for studying problems where the transition weights are expected to depend on the level of some specific switching variables. In comparison, our GSTVAR model facilitates capturing more complicated switching dynamics and results in more data-driven regimes. However, it is not always clear how to interpret the regimes economically, and due to the complexity of the transition weights, the estimation of the GSTVAR model can be tedious in practice.

Another popular branch of the literature on nonlinear VAR models focuses on so called Markov-switching VAR (MS-VAR) models (Krolzig, 1997, see also Hamilton, 1989, 1990). They incorporate discrete regime switches that are random and unobserved, and the switching probabilities depend on the preceding regime. The MS-VAR models can flexibly capture nonlinearities in the data, but unlike our GSTVAR model, they do not accommodate gradual shifts in the dynamics nor complicated switching dynamics.

We apply our GSTVAR model to study the macroeconomic effects of severe weather shocks and consider a monthly U.S. data set covering the period from 1961:1 to 2022:3 and containing an indicator of severe weather and a number of macroeconomic variables. We find

a specification with two regimes sufficient. The first regime mainly dominates the earlier part of the sample period, particularly during the volatile periods of 1970's and 1980's, but also prevails in the later sample during the Financial crisis and the COVID-19 crisis. The second regime dominates the latter part of the sample period. Following Kim, Mattheis, and Phan (2022), we identify the severe weather shock recursively, placing the the severe weather indicator first in the vector of variables. In both regimes, a positive severe weather shock decreases GDP, consumer prices, and the interest rate, but the effects are clearly stronger in the first regime prevailing in the earlier part of the sample period and in certain crisis periods. In contrast to Kim *et al.* (2022), we thus conclude that the effects of the severe weather shock are stronger in the earlier than the latter part of the sample, which suggests that the U.S. economy has adapted to the changing distribution of weather related shocks over time. However, the potential adaptation may not provide sufficient resilience when the economy is in a vulnerable state.

The rest of this paper is organized as follows. Section 2 first presents our framework for STVAR models, then discusses stationarity and ergodicity of the STVAR models. We also introduce the structural STVAR model and some tools useful in empirical analysis based on it. Finally, the Gaussian STVAR (GSTVAR) model is introduced by specifying the transition weights and the error distribution, and the GSTVAR model is compared to related models proposed in the previous literature. Section 3 discusses model selection and estimation of the parameters by the method of maximum likelihood. Section 4 presents the empirical application to the macroeconomic effects of severe weather shocks. Finally, Section 5 concludes. Further discussion on the stationarity condition and a Monte Carlo algorithm for estimating the generalized impulse response function (Koop, Pesaran, and Potter, 1996), as well as details on the empirical application are deferred to appendices. The introduced methods are implemented to the R package `sstvars` (Virolainen, 2024), available on an author's GitHub page <https://github.com/saviviro/sstvars>.

2 Smooth transition vector autoregressive models

2.1 General framework for STVAR models

The STVAR model with M regimes and autoregressive order p considered in this paper can be written as

$$y_t = \sum_{m=1}^M \alpha_{m,t} \mu_{m,t} + u_t, \quad u_t \sim (0, \Omega_{y,t}), \quad (2.1)$$

$$\mu_{m,t} = \phi_{m,0} + \sum_{i=1}^p A_{m,i} y_{t-i}, \quad m = 1, \dots, M, \quad (2.2)$$

$$\Omega_{y,t} = \sum_{m=1}^M \alpha_{m,t} \Omega_m, \quad (2.3)$$

where $\phi_{1,0}, \dots, \phi_{M,0} \in \mathbb{R}^d$, $m = 1, \dots, M$, are the intercept parameters, $A_{1,i}, \dots, A_{M,i} \in \mathbb{R}^{d \times d}$, $i = 1, \dots, p$, are the autoregressive matrices, and $\Omega_1, \dots, \Omega_M$ are the positive definite $(d \times d)$ covariance matrices of the regimes. The serially uncorrelated reduced form innovations u_t follow some distribution with zero mean and conditional covariance matrix $\Omega_{y,t}$. The transition weights $\alpha_{m,t}$ are assumed to be \mathcal{F}_{t-1} -measurable functions of $\{y_{t-j}, j = 1, \dots, p\}$ and to satisfy $\sum_{m=1}^M \alpha_{m,t} = 1$ at all t . These weights convey the relative proportions of the regimes at each point in time and determine how the process shifts between them. Specifically, when the process is completely in one of the regimes, the transition weight $\alpha_{m,t}$ of that regime equals unity, while the weights of the rest of the regimes are equal to zero. As the process begins a shift towards another regime, the transition weight of the emerging regime increases due to the dynamics captured in the transition weight function through the preceding observations. Concurrently, the weight of the previously dominant regime decreases.

It is easy to see that, conditional on \mathcal{F}_{t-1} , the conditional mean of the above-described process is $\mu_{y,t} \equiv E[y_t | \mathcal{F}_{t-1}] = \sum_{m=1}^M \alpha_{m,t} \mu_{m,t}$, and its conditional covariance matrix is

$\Omega_{y,t} = \text{Cov}(y_t | \mathcal{F}_{t-1}) = \sum_{m=1}^M \alpha_{m,t} \Omega_m$. That is, the conditional mean is a weighted sum the regime-specific means $\mu_{m,t}$ with the weights given by the transition weights $\alpha_{m,t}$, whereas the conditional covariance matrix is a weighted sum of the regime-specific conditional covariance matrices Ω_m .

We assume that the transition weights are functions of $\{y_{t-j}, j = 1, \dots, p\}$, which is required for applicability of the stationarity condition discussed below. We also assume that the transition weights are identical for all the individual equations in (2.1) and (2.3), which is also required for applicability of the stationarity condition. Consequently, at each t , the process can be described as a weighted sum of linear vector autoregressions. As discussed in Section 2.3.1, different STVAR models are obtained by specifying the transition weights or the error distribution in various ways. For instance, defining $\alpha_{2,t}$ as the logistic function and $\alpha_{1,t}$ as $1 - \alpha_{2,t}$ gives the two-regime logistic STVAR model popular in the empirical macroeconomic literature (see, e.g., Auerbach and Gorodnichenko, 2012), while transition weights like the mixing weights in Kalliovirta *et al.* (2016) yield the Gaussian STVAR model discussed in Section 2.3.

For standard asymptotic inference, the STVAR process must be stationary and ergodic. To verify that this is indeed the case, we rely on the sufficient condition for stationarity and ergodicity derived by Kheifets and Saikkonen (2020). However, their parametrization is not quite the same as ours, so their result must be slightly modified for our purposes (see Appendix A for details). In terms of the companion form AR matrices of the regimes defined as

$$\mathbf{A}_m = \begin{bmatrix} A_{m,1} & A_{m,2} & \cdots & A_{m,p-1} & A_{m,p} \\ I_d & 0 & \cdots & 0 & 0 \\ 0 & I_d & & 0 & 0 \\ \vdots & & \ddots & \vdots & \vdots \\ 0 & 0 & \cdots & I_d & 0 \end{bmatrix}, \quad m = 1, \dots, M, \quad (2.4)$$

$(dp \times dp)$

Kheifets and Saikkonen (2020, Theorem 1) show that if the following condition holds, the STVAR process is ergodic stationary (both strictly and second-order).

Condition 1. $\rho(\{\mathbf{A}_1, \dots, \mathbf{A}_M\}) < 1$.

Here

$$\rho(\mathcal{A}) = \limsup_{j \rightarrow \infty} \left(\sup_{A \in \mathcal{A}^j} \rho(A) \right)^{1/j}, \quad (2.5)$$

denotes the joint spectral radius (JSR) of a finite set of square matrices \mathcal{A} with $\mathcal{A}^j = \{A_1 A_2 \dots A_j : A_i \in \mathcal{A}\}$ and $\rho(A)$ is the spectral radius of the square matrix A . As Kheifets and Saikkonen (2020) note, Condition 1 is not necessary for ergodic stationarity of the process, meaning that if it does not hold, we just cannot use the result to state whether the process is ergodic stationary or not.

It is worth to mention that a necessary condition for the sufficient condition is that the usual stability condition is satisfied for each of the regimes since $\max(\rho(\mathbf{A}_1), \dots, \rho(\mathbf{A}_M)) \leq \rho(\{\mathbf{A}_1, \dots, \mathbf{A}_M\})$ (see Kheifets and Saikkonen, 2020, and the references therein). Therefore, the following condition, which is analogous to Corollary 1 of Kheifets and Saikkonen (2020), is necessary for Condition 1.

Condition 2. $\max\{\rho(\mathbf{A}_1), \dots, \rho(\mathbf{A}_M)\} < 1$.

Since the sufficient Condition 1 is computationally costly to verify with a reasonable accuracy (see, e.g., Chang and Blondel, 2013), it is useful to employ the more easily verified necessary Condition 2 in numerical estimation discussed in Section 3. As our estimation procedure produces a set of alternative local solutions, Condition 1 can be checked for each of them after the estimation, and the researcher can choose to use the best local solution whose stationarity can be verified.

A number of methods for bounding the JSR have been proposed in the literature, many of which are discussed by Chang and Blondel (2013). The accompanying R package `sstvars` (Virolainen, 2024) implements the branch-and-bound method of Gripenberg (1996). The JSR toolbox in MATLAB (Jungers, 2023), in turn, automatically combines various methods in the estimation of the JSR to enhance computational efficiency.

2.2 Structural STVAR model

To conduct structural analysis in the STVAR model, we need to find its structural counterpart involving orthogonal, serially uncorrelated structural errors, or shocks, e_t . This amounts to finding a non-singular ($d \times d$) impact matrix B_t such that the conditional covariance matrix of $e_t = B_t^{-1}u_t$, conditional on \mathcal{F}_{t-1} , is a diagonal matrix (typically normalized to the identity matrix). In other words, B_t must be such that $B_t^{-1}\Omega_{y,t}B_t'^{-1} = I_d$. However, without additional identifying restrictions B_t satisfying this equation is not unique, and as discussed by, e.g., Kilian and Lütkepohl (2017, Chapter 18), imposing such restrictions in nonlinear structural VAR models may not be straightforward. In our empirical application in Section 4, we consider a recursive model, where B_t is obtained by a lower-triangular Cholesky decomposition of the covariance matrix of the reduced-form residuals in each regime.

Conventional impulse responses can be computed separately for each regime in the structural STVAR model, as has been done in much of the nonlinear structural VAR literature. However, by thus precluding future regime switches, this approach changes the structure of the model and makes the impulse response analysis subject to Lucas critique. Moreover, the expected effects of the structural shocks generally depend on the initial values of the variables as well as the sign and size of the shock, which is not accounted for by the conventional impulse responses. However, the generalized impulse response function (GIRF) of Koop *et al.* (1996) can be used. The GIRF is defined as

$$\text{GIRF}(h, \delta_j, \mathcal{F}_{t-1}) = \mathbb{E}[y_{t+h}|\delta_j, \mathcal{F}_{t-1}] - \mathbb{E}[y_{t+h}|\mathcal{F}_{t-1}], \quad (2.6)$$

where h is the chosen horizon and $\mathcal{F}_{t-1} = \sigma\{y_{t-j}, j > 0\}$ as before. The first term on the right side of (2.6) is the expected realization of the process at time $t+h$ conditionally on a structural shock of sign and size $\delta_j \in \mathbb{R}$ in the j th element of e_t at time t and the previous observations. The latter term on the right side is the expected realization of the process conditionally on the

previous observations only. The GIRF thus expresses the expected difference in the future outcomes when the structural shock of sign and size δ_j in the j th element hits the system at time t as opposed to all shocks being random. An interesting feature of the structural STVAR model is that besides the generalized impulse response functions of the observable variables, it produces the GIRFs of the transition weights $\alpha_{m,t}$, $m = 1, \dots, M$, which yield information on the dynamic effects of the shocks on regime switches. They are obtained by replacing y_{t+h} with $\alpha_{m,t}$ on the right side of Equation (2.6).

It is easy to see that the GSTVAR model has a p -step Markov property, so conditioning on (the σ -algebra generated by) the p previous observations $\mathbf{y}_{t-1} = (y_{t-1}, \dots, y_{t-p})$ is effectively the same as conditioning on \mathcal{F}_{t-1} at time t and later. In order to estimate GIRFs conditional on that the economy is in a specific regime when the shock arrives, we generate initial values $\mathbf{y}_{t-1} = (y_{t-1}, \dots, y_{t-p})$ from the stationary distribution of that regime and the estimate GIRFs for each of these initial values. Taking the sample mean and quantiles over the estimated GIRFs then produces the point estimate and confidence bounds, respectively. Our confidence bounds thus reflect uncertainty about the initial state of the economy within the specific regime. A more detailed description of our Monte Carlo algorithm for estimating the GIRF is presented in Appendix B.

Similarly to the conventional impulse response functions being unsuitable for impulse response analysis in the structural STVAR model (due to their inability to capture asymmetries in the effects of the shocks or to take future switches in the regime into account), the conventional forecast error variance decomposition is unsuitable for tracking the relative contribution of each shock to the variance of the forecast errors. Instead, the generalized forecast error variance decomposition (GFEVD) of Lanne and Nyberg (2016) can be used. It is defined for variable i , shock j , and horizon h as

$$\text{GFEVD}(h, y_{it}, \delta_j, \mathcal{F}_{t-1}) = \frac{\sum_{l=0}^h \text{GIRF}(l, \delta_j, \mathcal{F}_{t-1})_i^2}{\sum_{k=1}^d \sum_{l=0}^h \text{GIRF}(l, \delta_k, \mathcal{F}_{t-1})_i^2}, \quad (2.7)$$

where h is the chosen horizon and $\text{GIRF}(l, \delta_j, \mathcal{F}_{t-1})_i$ is the i th element of the related GIRF. The GFEVD is otherwise similar to the conventional forecast error variance decomposition but with GIRFs in the place of conventional impulse response functions, and it can be interpreted in a similar manner to the conventional forecast error variance decomposition.

2.3 Gaussian STVAR model

Specifying a particular STVAR (and the related structural STVAR) model from the definition in Section 2.1 amounts to specifying the distribution of the reduced form innovations u_t (or the structural shocks e_t) and the transition weights $\alpha_{m,t}$. In this paper, we propose a Gaussian STVAR model with standard normal distributions for the structural errors e_t . Hence, the conditional distribution of y_t , conditional on \mathcal{F}_{t-1} , is Gaussian and characterized by the density function

$$f(y_t | \mathcal{F}_{t-1}) = n_d(y_t; \mu_{y,t}, \Omega_{y,t}) = (2\pi)^{-d/2} \det(\Omega_{y,t})^{-1/2} \exp \left\{ -\frac{1}{2}(y_t - \mu_{y,t})' \Omega_{y,t}^{-1} (y_t - \mu_{y,t}) \right\}. \quad (2.8)$$

That is, the conditional distribution is the d -dimensional Gaussian distribution with mean $\mu_{y,t}$ and covariance matrix $\Omega_{y,t}$.

The GSTVAR model has the advantage that, as the conditional distribution is Gaussian, the stationary distributions of the regimes corresponding to p consecutive observations are known, and, hence, the weighted relative likelihoods of the regimes can be used as transition weights. In this specification, the transition weights depend on the full distribution of the preceding p observations, and they are defined identically to the mixing weights of the GMVAR model (Kalliovirta *et al.*, 2016). Denoting $\mathbf{y}_{t-1} = (y_{t-1}, \dots, y_{t-p})$, the transition weights are defined as

$$\alpha_{m,t} = \frac{\alpha_m n_{dp}(\mathbf{y}_{t-1}; \mathbf{1}_p \otimes \mu_m, \Sigma_{m,p})}{\sum_{n=1}^M \alpha_n n_{dp}(\mathbf{y}_{t-1}; \mathbf{1}_p \otimes \mu_n, \Sigma_{n,p})}, \quad m = 1, \dots, M, \quad (2.9)$$

where $\alpha_1, \dots, \alpha_M$ are transition weight parameters that satisfy $\sum_{m=1}^M \alpha_m = 1$ and $n_{dp}(\cdot; \mathbf{1}_p \otimes \mu_m, \Sigma_{m,p})$ is the density function of the dp -dimensional normal distribution with mean $\mathbf{1}_p \otimes \mu_m$ and covariance matrix $\Sigma_{m,p}$. The symbol $\mathbf{1}_p$ denotes a p -dimensional vector of ones, \otimes is Kronecker product, $\mu_m = (I_d - \sum_{i=1}^p A_{m,i})^{-1} \phi_{m,0}$, and the covariance matrix $\Sigma_{m,p}$ is given in Lütkepohl (2005, Equation (2.1.39)), but using the parameters of the m th regime. In other words, $n_{dp}(\cdot; \mathbf{1}_p \otimes \mu_m, \Sigma_{m,p})$ corresponds to the density function of the stationary distribution of the m th regime.

The transition weights are thus weighted ratios of the stationary densities of the regimes corresponding to the preceding p observations. The specification of the transition weights is appealing, as it states that the greater the weighted relative likelihood of a regime is, the greater the weight of this regime is. The regimes are, hence, formed based on the statistical properties of the data and are not affected by the choice of switching variables. This is a convenient feature for forecasting, and it also facilitates associating statistical characteristics and economic interpretations to the regimes.

2.3.1 Comparison to related models

Our GSTVAR model has a number of desirable features compared to popular alternative nonlinear VAR models. As already discussed, in line with the GMVAR model of Kalliovirta *et al.* (2016), the transition between the regimes depends on multiple past observations in contrast to the Markov-switching VAR (MS-VAR) model, where the transition probabilities depend on the most recent regime, or the logistic STVAR (LSTVAR) and threshold VAR (TVar) models, where the regime is determined by the lagged value of an observable variable or an exogenous switching variable. On the other hand, like the LSTVAR model, the GSTVAR model facilitates gradual shifts between the regimes, whereas in the TVar, GM-VAR and MS-VAR models each observation is generated from a single regime. Hence, the GSTVAR model combines the advantages of the GMVAR, TVar, LSTVAR and MS-VAR

models.

Although the transition weight function of the GSTVAR model is similar to the mixing weights of the GMVAR model, it differs from that model in other ways. Specifically, the GMVAR model generates each observation from a randomly selected distinct regime, while the GSTVAR model allows for smooth transitions between the regimes and thereby facilitates gradual shifts in the dynamics. This is the case because in the GMVAR model, the transition weights $\alpha_{m,t}$ are replaced by unobservable regime variables $s_{m,t}$ in Equations (2.1)–(2.3). These regime variables $s_{m,t}$, $m = 1, \dots, M$, are such that at each t , exactly one of them takes the value one, whereas the rest take value zero according to the probabilities $P(s_{m,t} = 1 | \mathcal{F}_{t-1}) = \alpha_{m,t}$. Because the regime that generates each observation is thus unknown in the GMVAR model, the (structural) errors cannot, in general, be recovered from the data, while they are readily available in the GSTVAR model. This is particularly important in structural analysis because it enables computing the historical decomposition and conducting counterfactual analyses.

The LSTVAR model is a particular STVAR model with logistic transition weights, originally introduced to VAR models in Anderson and Vahid (1998). A simple two-regime ($M = 2$) logistic STVAR model commonly considered in the previous literature is obtained by defining the transition weights as

$$\alpha_{1,t} = 1 - \alpha_{2,t}, \quad \alpha_{2,t} = [1 + \exp\{-\gamma(y_{i,t-j} - c)\}]^{-1}, \quad (2.10)$$

where $y_{i,t-j}$ is the j th lagged observation ($j \in \{1, \dots, p\}$) of the i th variable ($i \in \{1, \dots, d\}$), $c \in \mathbb{R}$ is a location parameter, and $\gamma > 0$ is a scale parameter. The location parameter c determines the mid-point of the transition function, i.e., the value of the switching variable when the weights are equal. The scale parameter γ , in turn, determines the smoothness of the transitions (smaller γ implies smoother transitions), and it is assumed strictly positive so that $\alpha_{2,t}$ is increasing in $y_{i,t-j}$. This simple setup can be generalized in various directions (see, e.g.,

Teräsvirta and Yang, 2014). It is also possible to use an exogenous or deterministic switching variable instead of a lagged endogenous variable in the logistic transition weights (2.10). However, in these cases, it may be difficult to determine whether the model is stationary, and it is not generally possible to estimate the true nonlinear generalized impulse response functions.

The logistic transition weights have the advantage that the regimes typically have clear interpretations and the switching variable can be defined to address some specific aspect of the empirical problem. For example, when using the lagged GDP growth as the switching variable, the regimes can be interpreted as recession and expansion. In comparison, the transition weights of the GSTVAR model depend on the full distribution of the preceding p observations and can thereby capture more complicated switching-dynamics, which facilitates associating the different regimes with different aspects of the phenomenon being modelled. As the transition weights of the GSTVAR model are not affected by the choice of a switching variable but determined based on the weighted relative likelihoods of the regimes, they are more clearly data-driven and their own evolution is interesting as such. However, the resulting regimes are statistically determined, so it is not always clear how to interpret them in terms of a given application.

The threshold VAR (TVAR) model (Tsay, 1998) is otherwise similar to the LSTVAR model, but the regime switches are discrete. It is obtained as a special case of the STVAR model of Section 2.1 by assuming

$$\alpha_{m,t} = I(c_{m-1} < s_t < c_m), \quad m = 1, \dots, M, \quad (2.11)$$

in Equation (2.1), where $I(\cdot)$ is an indicator function, s_t is the switching variable at the time t , and $-\infty < c_1 < \dots < c_M < \infty$ are threshold parameters. When $s_t = y_{it-j}$ for some variable $i \in \{1, \dots, d\}$ and lag $j \in \{1, \dots, p\}$, the model is called the self-exciting TVAR model.

The MS-VAR model, introduced by Krolzig (1997) (see also Hamilton, 1990), is quite similar to the GMVAR model of Kalliovirta *et al.* (2016) with the exception that the switching-probabilities depend on the preceding regime only. In contrast to STVAR models, regime-switches in the MS-VAR model are discrete and unobserved. Specifically, the MS-VAR model is obtained from Equations (2.1)–(2.3) by replacing the transition weights $\alpha_{m,t}$ with unobservable regime variables $s_{m,t}$, $m = 1, \dots, M$, such that at each t , exactly one of them takes the value one and the others take value zero. The regime variable that takes the value one is selected randomly according to the probabilities

$$P(s_{m,t} = 1 | s_{n,t-1} = 1) = p_{mn} \text{ for all } t \text{ and } m, n = 1, \dots, M, \quad (2.12)$$

that satisfy $\sum_{n=1}^M p_{mn} = 1$ for all m . In other words, the regime that generates each observation is selected randomly at each t according to the probabilities p_{mn} , $m, n = 1, \dots, M$. While the MS-VAR model is a relatively simple framework for flexibly modelling nonlinear time series with unobservable discrete regime-switches, unlike our GSTVAR model, it is unable to capture gradual shifts in the dynamics of the data. Moreover, in the same way as in the GMVAR model, it is not possible to recover structural shocks from the fitted model because the regime that generates each observation is not observed.

3 Estimation and model selection

3.1 Maximum likelihood estimation

The parameters of the GSTVAR model can be estimated by the method of maximum likelihood (ML). We collect the parameters to the vector

$$\boldsymbol{\theta} = (\phi_{1,0}, \dots, \phi_{m,0}, \varphi_1, \dots, \varphi_M, \sigma, \alpha), \quad (3.1)$$

where $\varphi_m = (\text{vec}(A_{m,1}), \dots, \text{vec}(A_{m,p}))$, $m = 1, \dots, M$, $\sigma = (\text{vech}(\Omega_1), \dots, \text{vech}(\Omega_M))$, $\alpha = (\alpha_1, \dots, \alpha_{M-1})$ contains the transition weight parameters (notice that $\alpha_M = 1 - \sum_{m=1}^{M-1} \alpha_m$).

Indexing the observed data as $y_{-p+1}, \dots, y_0, y_1, \dots, y_T$, the conditional log-likelihood function, conditional on the initial values $\mathbf{y}_0 = (y_0, \dots, y_{-p+1})$, is given as

$$L_t(\boldsymbol{\theta}) = \sum_{t=1}^T l_t(\boldsymbol{\theta}) = \sum_{t=1}^T \log n_d(y_t; \mu_{y,t}, \Omega_{y,t}). \quad (3.2)$$

where $n_d(y_t; \mu_{y,t}, \Omega_{y,t})$ is the d -dimensional conditional density of the process, conditional on \mathcal{F}_{t-1} , at time t , given in Equation (2.8). Hence, the ML estimator of $\boldsymbol{\theta}$ maximizes the log-likelihood function $L_t(\boldsymbol{\theta})$ over the parameter space specified below.

To ensure ergodic stationarity of the process, we assume that Condition 1 in Section 2.1 holds. Moreover, it is assumed that the true parameter value is an interior point of a compact subset of the parameter space, which is a standard condition for asymptotic normality of the ML estimator. Thus, given ergodic stationarity of the process, there is no particular reason to believe that the standard asymptotic results of consistency and asymptotic normality would not apply to the ML estimator. Finally, to achieve identification of the parameters such that the regimes cannot 'relabelled' to obtain the same model with different parameter vectors, we order the transition weight parameters α_m , $m = 1, \dots, M$ in a decreasing order. That is, we assume

$$\alpha_1 > \dots > \alpha_M \text{ and } (\phi_{m,0}, \varphi_m, \text{vech}(\Omega_m)) \neq (\phi_{n,0}, \varphi_n, \text{vech}(\Omega_n)) \text{ for } m \neq n \in \{1, \dots, M\}. \quad (3.3)$$

The constraints imposed on the parameter space are summarized in the following assumption.

Assumption 1. *The true parameter value $\boldsymbol{\theta}_0$ is an interior point of $\boldsymbol{\Theta}$, which is a compact subset of the parameter space $\{\boldsymbol{\theta} = (\phi_{1,0}, \dots, \phi_{m,0}, \varphi_1, \dots, \varphi_M, \sigma, \alpha, \nu) \in \mathbb{R}^{M(d+d^2p+d(d+1)/2)} \times (0, 1)^{M-1} \times (2, \infty) : \Omega_m \text{ is positive definite for all } m = 1, \dots, M, \text{ and Conditions 1 and (3.3) hold.}\}$*

Finding the ML estimate amounts to maximizing the log-likelihood function in (3.2) over a high dimensional parameter space satisfying the constraints in Assumption 1. Due to the complexity of the log-likelihood function, numerical optimization methods are required. The maximization problem can, however, be challenging in practice due to the complicated dependence of the transition weights on the preceding observations, which induces a large number of modes to the surface of the log-likelihood function, and large areas to the parameter space, where it is flat in multiple directions.

We follow Virolainen (2022, forthcoming) and Meitz, Preve, and Saikkonen (2023) and employ a two-phase estimation procedure that is ran for a large number of times. In the first phase, a genetic algorithm is used to find parameter values that are near local maximum points of the log-likelihood function. Since genetic algorithms tend to converge slowly near local solutions, a gradient based variable algorithm is ran for each of the starting values, resulting in a number of alternative local solutions. Some of the estimation rounds may end up in saddle points or near-the-boundary points that are not local solutions, and some of the local solutions may be inappropriate for statistical inference (for instance, there might be only few observations from some of the regimes). Because Condition 1 included in Assumption 1 is computationally costly to verify, we recommend using the necessary Condition 2 to restrict the parameter space.

After the estimation rounds have been ran, the researcher can choose among the appropriate local solutions the one that maximizes the log-likelihood. Then, the sufficient Condition 1 for ergodic stationarity can be checked for the selected local solution if the more easily verified necessary Condition 2 is used to restrict the parameter space instead of Condition 1 in the estimation. The accompanying R package `sstvars` employs a modified genetic algorithm that works similarly to the one described in Virolainen (2022).

3.2 Model selection

To select the number of regimes and the autoregressive order of the GSTVAR model, a suitable strategy is to start with a relatively simple specification and then build up to more complicated models if necessary. In particular, it may be useful to begin with linear Gaussian VAR models (i.e., GSTVAR models with only one regime) to evaluate to what extent they can capture the relevant characteristics of the data. Then, the order of the model or the number of regimes can be increased, if needed.

It is well known that testing for linearity against a model with multiple regimes, in general, poses a nonstandard testing problem because the model is identified only under the alternative (Davies, 1977). This is the case also in our setup, and, therefore, we follow the previous literature and recommend using information criteria and residual-based diagnostic checks to compare the fit of models with different orders and numbers of regimes, as well as to study their adequacy in capturing the autocorrelation structure, conditional heteroskedasticity, and distribution of the data. The derivation of formal diagnostic tests is beyond the scope of this paper, but graphical devices, including quantile-quantile plots as well as autocorrelation and cross-correlation functions of the residuals and their squares, can be used to this end.

For a number of reasons, GSTVAR models of a relatively low autoregressive order are preferable. Firstly, the estimation of GSTVAR models with a large p can be tedious in practice. Secondly, if the order p is large, the number of parameters increases vastly when the number of regimes is increased, which substantially decreases estimation accuracy. Thirdly, unlike in linear VARs, decreasing the autoregressive order may actually improve the fit because the transition weights are calculated using the whole joint distribution of the preceding p observations. Consequently, the sensitivity of the transition weights to individual observations and, hence, responsiveness to changes in the dynamics of the data decrease with p .

It is also advisable to be conservative with the number of regimes M because if the number

of regimes is chosen too large, some of the parameters in the model are not identified (see the related discussion in Kalliovirta *et al.*, 2016, Section 3.4). Moreover, increasing the number of regimes substantially increases the complexity of the surface of the log-likelihood function, making the estimation of the parameters challenging in practice.

4 Empirical application

In this section, we apply our GSTVAR model to study the effects of severe weather on the U.S. macroeconomy. This issue has previously been addressed by Kim *et al.* (2022), who employ a two-regime recursive STVAR model with transition weights defined by a linear time trend ($\alpha_{2,t} = t/T$ and $\alpha_{1,t} = 1 - \alpha_{2,t}$). They argue that allowing for time-varying coefficients in the model is important because the economic effects of severe weather may have changed due to actions potentially taken for the economy to adapt to climate change. According to Kim *et al.* (2022), there is little evidence in favor of adaptation to severe weather in the U.S., as the impacts of the severe weather shocks are found significant only towards the end of the sample (spanning from 1963 to 2019).

The linear time trend might not, however, sufficiently describe the adaptation of the economy, because the effects of severe weather may vary across different states of the economy due to variation in factors such as fiscal flexibility and sector-specific vulnerabilities. It is not obvious how such variation should be accommodated in the transition weights in a nonlinear SVAR model. We address this issue with our GSTVAR model in which the regimes and shifts between them are formed based on the statistical properties of the data through the full distribution of the preceding p observations. This approach plausibly better describes the evolution of the joint dynamics of severe weather and U.S. macroeconomy through time than an STVAR model with transition weights defined by a linear time trend.

4.1 Data

We consider a four-variable monthly U.S. data set that covers the period from 1961:1 to 2022:3 ($T = 735$ observations) and includes indicators for severe weather and economic activity as well as consumer price inflation and an interest rate variable. As argued by Kim *et al.* (2022), it is important to use data of more high frequency than quarterly because some weather effects can be short-lived, and the end point of our sample period is determined by the availability of the monthly GDP growth data. While the sample period is slightly longer than in Kim *et al.* (2022), our general conclusions are not affected by using their shorter sample period (from 1963:4 to 2019:5), as discussed in Appendix C.2.

As an indicator of the frequency of severe weather and the extent of sea level rise, we use the Actuaries Climate Index (ACI), developed by actuarial organizations in the United States and Canada (American Academy of Actuaries, Canadian Institute of Actuaries, Casualty Actuarial Society, and Society of Actuaries, 2023). Following Kim *et al.* (2022), we seasonally adjust the ACI series with the standard Census Bureau X-13 seasonal adjustment algorithm. For a more detailed description of ACI, see Kim *et al.* (2022).

As an aggregate measure of real economic activity, we use the monthly GDP growth rate constructed by the Federal Reserve Bank of Chicago from a collapsed dynamic factor analysis of a panel of 500 monthly measures of real economic activity and quarterly real GDP growth (Federal Reserve Bank of Chicago, 2023). While Kim *et al.* (2022) use both the industrial production index and unemployment rate to measure real economic activity at the monthly frequency, we opt for the monthly GDP growth rate instead. It has the advantage of being a more comprehensive measure of real economic activity, including agricultural output, tourism, and services, which can be significantly affected by the severe weather shocks.

Finally, we include the monthly growth rate of the consumer price index (CPI) and the effective federal funds rate that is replaced by the Wu and Xia (2016) shadow rate for the

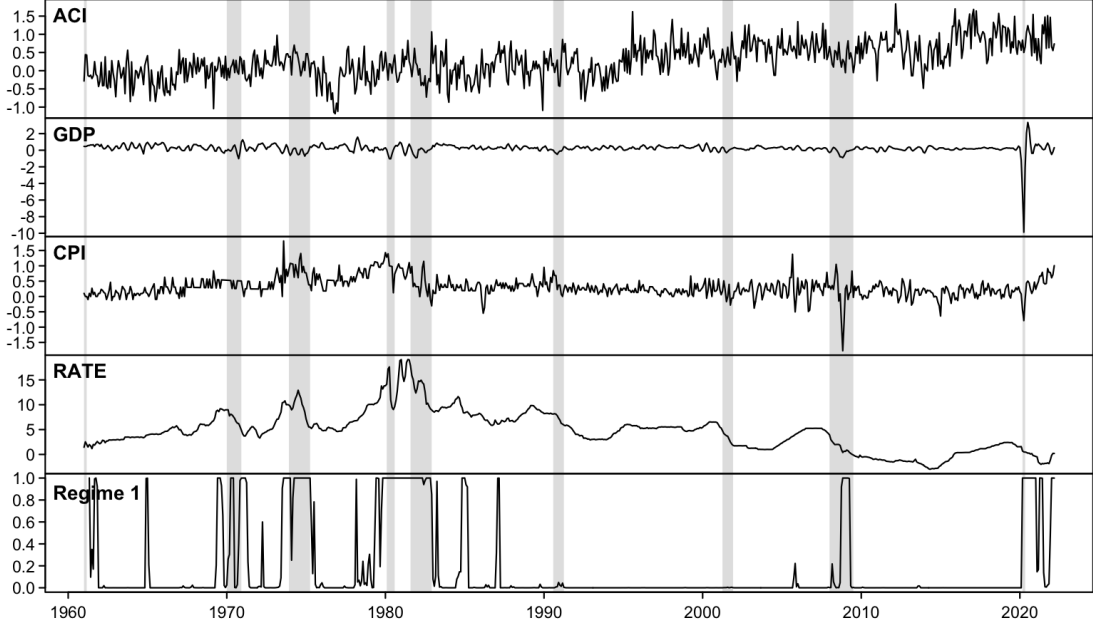


Figure 1: Monthly U.S. time series covering the period from 1961:1 to 2022:3. From top to bottom, the variables are the Actuaries Climate Index, the monthly GDP growth rate, the monthly CPI growth rate, and the effective federal funds rate (replaced by the Wu and Xia (2016) shadow rate for the zero lower bound periods). The bottom panel shows the estimated transition weights of the first regime of the fitted two-regime fourth-order GSTVAR model. The shaded areas indicate the U.S. recessions defined by the NBER.

zero lower bound periods. The CPI and federal funds rate series were downloaded from the Federal Reserve Bank of St. Louis database and Wu and Xia (2016) shadow rate from the Federal Reserve Bank of Atlanta database. The time series are presented in the top four panels of Figure 1, where the shaded areas indicate the U.S. recessions defined by the NBER.

4.2 GSTVAR model

To select the order of our GSTVAR model, we start by examining the partial autocorrelation functions of the U.S. time series (shown in Figure C.1 of Appendix C). They suggest that the autoregressive order $p = 4$ could be reasonable for a parsimonious model. Therefore, we fit two-regime GSTVAR models with autoregressive orders $p = 1, \dots, 5$ and, to compare them, compute the values of three information criteria (AIC, BIC and HQIC). As seen

Model	Log-lik	BIC	HQIC	AIC
$p = 1, M = 1$	-1.755	3.780	3.665	3.593
$p = 2, M = 1$	-1.460	3.334	3.157	3.046
$p = 3, M = 1$	-1.411	3.381	3.142	2.992
$p = 4, M = 1$	-1.376	3.456	3.155	2.966
$p = 5, M = 1$	-1.355	3.560	3.197	2.968
$p = 1, M = 2$	-0.548	1.645	1.410	1.263
$p = 2, M = 2$	-0.220	1.277	0.919	0.694
$p = 3, M = 2$	-0.181	1.489	1.007	0.704
$p = 4, M = 2$	-0.121	1.658	1.052	0.671
$p = 5, M = 2$	-0.130	1.968	1.237	0.778

Table 1: The values of the log-likelihood function and the information criteria divided by the number of observations ($735 - p$) for a number of linear VAR and two-regime GSTVAR models.

in Table 1, the order $p = 4$ minimizes the AIC, whereas the order $p = 2$ minimizes the HQIC and BIC. The table also contains similar results for linear VAR (i.e., one-regime GSTVAR) models. In terms of the information criteria, they are clearly inferior to our two-regime GSTVAR models. While adding a third regime to the model might improve the fit, the number of parameters would be large compared the number of observations from each regime, substantially decreasing estimation accuracy. Moreover, since incorporating too many regimes in the model would also result in identification issues (see Section 3.2), we confine ourselves to two-regime models.

Based on graphical residual diagnostics, presented in Appendix C, the two-regime GSTVAR model with $p = 4$ lags captures the autocorrelation structure of the data reasonably well. Some of the conditional heteroskedasticity and marginal distribution of the series are not captured, but the inadequacies are not particularly severe. Finally, the sufficient Condition 1 for ergodic stationarity holds for the selected model, which is seen by finding an upper bound of the joint spectral radius of the matrices \mathbf{A}_m (2.4), $m = 1, 2$. with the JSR toolbox (Jungers, 2023) in MATLAB. The resulting upper bound is 0.995, which is strictly smaller than one, satisfying the stationary condition. Hence, we proceed with the two-regime fourth-order model.

The estimated transition weights indicate the relative importance of each regime, and the

time series of the weights of Regime 1 are presented in the bottom panel of Figure 1. The corresponding weights of Regime 2 are, of course, obtained by subtracting these weights from unity. It is not straightforward to give the regimes an economic interpretation. Regime 1 mainly dominates in the 1960’s, 1970’s, and 1980’s, but obtains large weights also during the Financial crisis and from the beginning of the COVID-19 crisis onwards (excluding a short period in 2021). Overall, Regime 1 thereby mostly prevails in the earlier sample and Regime 2 in the later sample. The dominance of Regime 1 during the volatile periods of 1970’s and 1980’s as well as during the Financial crisis and the COVID-19 crisis, suggests that it could, to some extent, represent more turbulent times compared to the second regime.

We are predominantly interested in the economic impact of severe weather, and, therefore, a severe weather shock (ACI shock) must be identified. This amounts to imposing a unique structure of the impact matrix B_t in (2.3) governing the contemporaneous relationships of the shocks, so that one of the shocks can be labelled the ACI shock. Following Kim *et al.* (2022), our key identification restriction is that the ACI shock is the only shock that can instantaneously affect the ACI index. This identification restriction seems reasonable, as it states that the other (macroeconomic) shocks do not affect severe weather or sea level within a month, but allows them to affect the ACI in the long run. We establish the identification by placing the ACI index first in the vector of variables and imposing a recursive lower-triangular structure on the impact matrix B_t , obtained by the Cholesky decomposition of the estimated conditional error covariance matrix $\Omega_{y,t}$.

4.3 Impulse response analysis

To study the effects of the ACI shock, we compute the generalized impulse responses of the variables to it. As pointed out in Section 2.2, due to the endogenously determined transition weights and the fact that we allow the regime to switch as a result of a shock, there are multiple types of possible asymmetries. Therefore, we compute generalized impulse

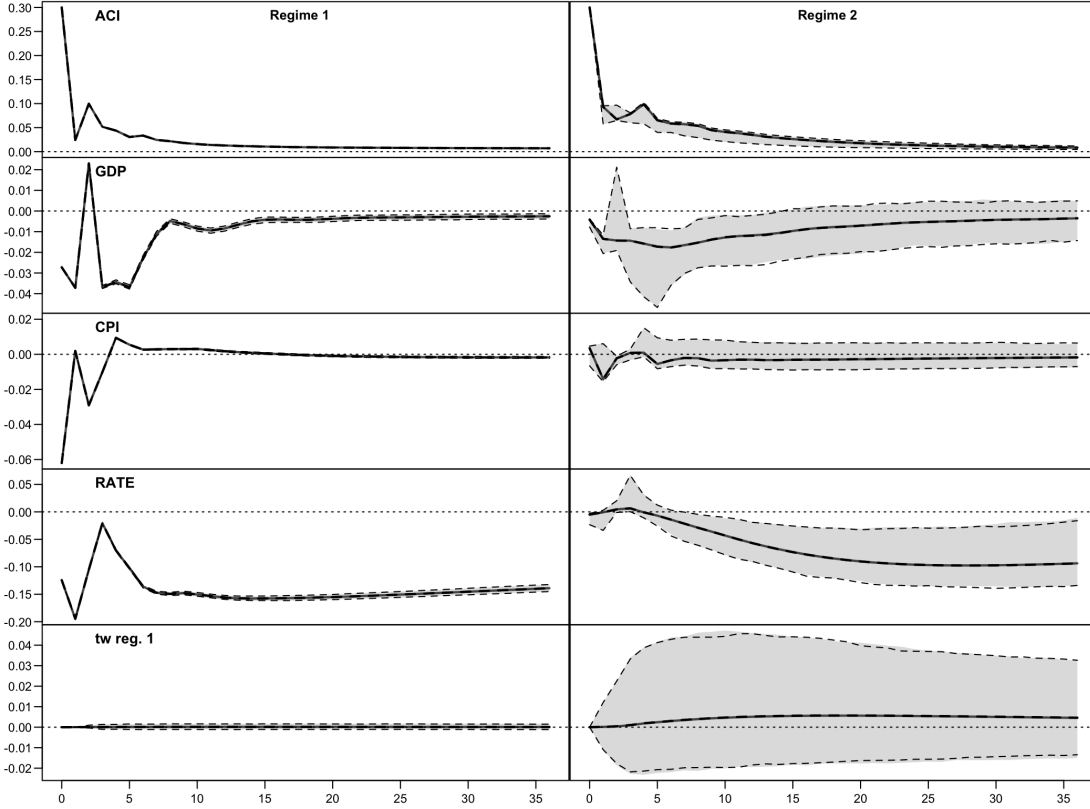


Figure 2: Generalized impulse response functions to the identified ACI shock $h = 0, 1, \dots, 36$ months ahead. From top to bottom, the responses of the ACI index, GDP growth rate, inflation growth rate, the interest rate variable, and transition weights of Regime 1 are depicted in each row. The left column shows the responses to a positive (grey solid line) and negative (black dashed line) one-standard-error shocks with initial values generated from the stationary distribution of Regime 1. The right column shows the corresponding responses in Regime 2. All GIRFs have been scaled so that the instantaneous change in the ACI index is 0.3. For a positive ACI shock, the 95% confidence intervals are depicted with shaded grey areas, whereas for a negative ACI shock, they are depicted as black dashed lines. The results are based on 2500 draws of initial values (for details of the algorithm, see Appendix B).

responses that can vary depending on the initial values of the variables as well as on the sign and size of the shock. We are particularly interested in finding out about the potential state-dependence of the effects of the ACI shock, and to capture them, we draw initial values from the stationary distribution of each regime separately. Shocks of different size seem to result in similar impulse responses, so we only report results for one standard-error shocks. The GIRFs are scaled so that the instantaneous response of the ACI index is 0.3, making the responses to shocks of different signs and sizes comparable.

Figure 2 presents the GIRFs (and the 95% confidence intervals) of the variables, including the transition weights, to the identified ACI shock $h = 0, 1, \dots, 36$ quarters ahead. The right and left columns depict the responses to a one-standard-error positive and negative shocks in Regime 1 and Regime 2, respectively. In both regimes, a positive ACI shock mainly decreases (and a negative shock increases) GDP, consumer prices, and the interest rate. However, there is a major difference in the GIRFs between the regimes: the effects of the ACI shock on all macroeconomic variables are clearly stronger in Regime 1. This may be the case because this regime appears to be attributed to more volatile times, including recessions and crisis periods. Thus, it might represent a state of the economy that is more vulnerable to weather related shocks, and therefore, a similar shock is likely to result in greater damage in Regime 1 than in Regime 2. Other differences between the regimes are small.

The 95% confidence intervals depicted in Figure 2 convey the uncertainty about the initial state of the economy within each regime, as explained in Section 2.2. Hence, the very narrow confidence intervals in Regime 1 indicate only very weak dependence of the GIRFs on the initial values in that regime. This is because the ACI shock has almost no effect on the transition weights of Regime 1, as shown in the bottom left panel of Figure 2, and thereby the GIRFs resemble linear IRFs computed for this regime. In Regime 2, on the other hand, the confidence intervals are wider, implying some variation in the GIRFs depending on the initial values within the regime.

As Regime 1 dominates the earlier part and Regime 2 is predominant in the latter part of the sample, we can conclude that the effect of severe weather shocks has diminished over time. This suggests that the U.S. economy has adapted to the effects of climate change. In contrast, Kim *et al.* (2022) found the effects of the ACI shock stronger at the end than at the beginning of their sample period from 1963:4 to 2019:5, which they interpret as insufficient adaptation in the U.S. economy to the changing distribution of weather related shocks.¹

¹ To check the robustness of our findings to the sample period, we also considered the subsample from 1963:4 to 2019:5 studied by Kim *et al.* (2022) and found the regimes of the fitted GSTVAR model quite similar to

While our results are thus, in general, contradictory to theirs, there are some short periods in the latter part of our sample where Regime 1 with stronger impact of the ACI shock prevails. These particularly overlap with the major crises, which suggests that the potential adaptation may not provide sufficient resilience against weather related shocks in a turbulent state of the economy.

To evaluate the relative importance of the ACI shock in each regime, we compute the GFEVD for each regime separately based on the estimated generalized impulse responses. The relative contributions of the positive one-standard-error ACI shock to the forecast error variance at various horizons are presented in Table 4.3. The ACI shock dominates the ACI index, while the relative importance of the other shocks increases at longer horizons, especially in Regime 1. However, its importance for the macroeconomic variables is minor. In Regime 1, its relative contribution to movements in GDP growth is smaller than in Regime 2, which may follow from the fact that in this more turbulent regime, characterized by recessions and crises, presumably other shocks prevail that are more dominant drivers of the macroeconomy. The last two rows of Table 4.3 show that the relative importance of the ACI shock for the transition weights is small in Regime 1 but quite substantial in Regime 2. This suggests that the severe weather shocks may have some importance in the state of economy when the economy is in the more tranquil Regime 2, while the transition from the more turbulent Regime 1 towards Regime 2 is mainly driven by other shocks.

5 Conclusion

We have introduced a Gaussian smooth transition vector autoregressive (GSTVAR) model with transition weights adopted from the Gaussian mixture VAR (GMVAR) model of Kalliovirta

our main specification. Also, the estimated GIRFs and main conclusions from them are similar, with the exception that the interest rate variable increases in response to a positive ACI shock in Regime 1. The details and figures of the transition weights and GIRFs are presented in Appendix C.2.

		$h = 0$	$h = 3$	$h = 6$	$h = 12$	$h = 24$	$h = 36$
ACI	Regime 1	100.00%	91.54%	87.24%	80.82%	69.76%	62.27%
	Regime 2	100.00%	98.96%	96.82%	95.80%	93.45%	91.10%
GDP	Regime 1	0.16%	0.44%	0.69%	0.71%	0.73%	0.74%
	Regime 2	0.10%	1.10%	2.47%	3.95%	5.00%	5.29%
CPI	Regime 1	5.40%	3.58%	3.24%	3.07%	3.01%	3.00%
	Regime 2	0.04%	0.59%	0.65%	0.75%	0.96%	1.06%
RATE	Regime 1	1.93%	1.18%	1.14%	1.61%	2.14%	2.38%
	Regime 2	0.08%	0.03%	0.05%	0.66%	2.88%	4.46%
$\alpha_{1,t}$	Regime 1		0.31%	0.80%	1.36%	1.48%	1.26%
	Regime 2		3.32%	13.45%	23.88%	29.69%	29.40%

Table 2: The relative contribution of the ACI shock to the forecast error variances of the variables in each regime at the horizons $h = 0, 3, 6, 12, 24, 36$ based on the generalized forecast error variance decompositions in each regime. The relative contribution to the transition weights $\alpha_{1,t}$ is not defined (and thereby not shown) at impact, because the transition weights are \mathcal{F}_{t-1} -measurable.

et al. (2016). Specifically, the transition weights of the GSTVAR model are constructed so that the greater the relative weighted likelihood of a regime is, the greater its transition weight is, which facilitates associating statistic characteristics and economic interpretations to the regimes. In other words, the GSTVAR model allows to capture gradual shifts in the dynamics of the data with switching dynamics that, for a p th order model, depend of the full distribution of the preceding p observations.

By making use of the results of Saikkonen (2008) and Kheifets and Saikkonen (2020), we presented a sufficient condition for stationarity and ergodicity of the GSTVAR model. We also discussed estimation of the model parameters by the method of maximum likelihood, which, due the complexity of the log-likelihood function, can be very tedious in practice. Hence, following Meitz *et al.* (2023) and Virolainen (2022, forthcoming), we proposed employing a two-phase procedure in which a genetic algorithm is used to find starting values for a gradient based method. The introduced methods, including a modified version of a genetic algorithm, are implemented to the R package `sstvars`, available on an author's GitHub page <https://github.com/saviviro/sstvars>.

We have applied our method to study the macroeconomic effects of severe weather shocks.

Our monthly data set covers the period from 1961:1 to 2022:3 and contains an indicator of the frequency of severe weather and the extent of sea level rise in addition to a number of macroeconomic variables. Our structural GSTVAR model has two regimes. Regime 1 mainly dominates the earlier part of the sample period, particularly the turbulent times of 1970's and 1980's, but also prevails in the later sample during the Financial crisis and the COVID-19 crisis, while the Regime 2 dominates the latter part of the sample period. Following Kim *et al.* (2022), we identified the severe weather shock recursively, placing the severe weather indicator first in the vector of variables. A positive weather shock was found to decrease GDP, consumer prices, and the interest rate in both regimes, but the effects are stronger in Regime 1. This finding contradicts the main result of Kim *et al.* (2022), who found the impacts of the weather shock to get stronger over time, interpreting this as lack of adaptation to changing weather. In contrast, our findings suggest that the U.S. economy has adapted to the changing distribution of weather related shocks. However, the adaptation may not provide sufficient resilience when the economy is in a vulnerable state.

References

American Academy of Actuaries, Canadian Institute of Actuaries, Casualty Actuarial Society, Society of Actuaries (2023). “Actuaries climate index.”

Anderson H., Vahid F. (1998). “Testing multiple equation systems for common nonlinear components.” *Journal of Econometrics*, **84**(1), 1–36.

Auerbach A. J., Gorodnichenko Y. (2012). “Measuring the output responses to fiscal policy.” *American Economic Journal: Economic Policy*, **4**(2), 1–27.

Chang C.-T., Blondel V. (2013). “An experimental study of approximation algorithms for the joint spectral radius.” *Numerical Algorithms*, **64**, 181–202.

Davies R. B. (1977). “Hypothesis testing when a nuisance parameter is present only under the alternative.” *Biometrika*, **64**, 247–254.

Federal Reserve Bank of Chicago (2023). “Monthly GDP growth rate data (<https://www.chicagofed.org/publications/bbki/index>).”

Gripenberg G. (1996). “Computing the joint spectral radius.” *Linear algebra and its applications*, **234**, 43–60.

Hamilton J. D. (1989). “A new approach to the economic analysis of nonstationary time series and the business cycle.” *Econometrica*, **57**(2), 357–384.

Hamilton J. D. (1990). “Analysis of time series subject to changes in regime.” *Journal of Econometrics*, **45**(1-2), 39–70.

Hubrich K., Teräsvirta T. (2013). “Thresholds and smooth transitions in vector autoregressive models.” *CREATES Research Paper 2013-18, Aarhus University*.

Jungers R. (2023). “The JSR toolbox (<https://www.mathworks.com/matlabcentral/fileexchange/33202-the-jsr-toolbox>), matlab central file exchange.”

Kalliovirta L., Meitz M., Saikkonen P. (2016). “Gaussian mixture vector autoregression.” *Journal of Econometrics*, **192**(2), 465–498.

Kheifets I., Saikkonen P. (2020). “Stationarity and ergodicity of vector STAR models.” *Econometric Reviews*, **39**(407–414), 1311–1324.

Kilian L., Lütkepohl H. (2017). “Structural vector autoregressive analysis.” 1st edition. Cambridge University Press, Cambridge.

Kim H., Matthess C., Phan T. (2022). “Severe weather and the macroeconomy.” *Working paper 21-14R, Federal Reserve Bank of Richmond*.

Koop G., Pesaran M., Potter S. (1996). “Impulse response analysis in nonlinear multivariate models.” *Journal of Econometrics*, **74**(1), 119–147.

Krolzig H.-M. (1997). “Markov-switching vector autoregressions - modelling, statistical inference, and application to business cycle analysis.” In H Dawid, A Kleine (eds.), *Lecture Notes in Econometrics and Mathematical Systems*, volume 454, chapter 1, pp. 6–28. Springer Berlin, Heidelberg, Berlin.

Lanne M., Nyberg H. (2016). “Generalized forecast error variance decomposition for linear and nonlinear multivariate models.” *Oxford Bulletin of Economics and Statistics*, **78**(4), 595–603.

Lütkepohl H. (2005). “New introduction to multiple time series analysis.” 1st edition. Springer, Berlin.

Meitz M., Preve D., Saikkonen P. (2023). “A mixture autoregressive model based on Student’s t -distribution.” *Communications in Statistics - Theory and Methods*, **52**(2), 499–515.

Saikkonen P. (2008). “Stability of regime switching error correction models under linear cointegration.” *Econometric Theory*, **24**(1), 294–318.

Teräsvirta T., Yang Y. (2014). “Specification, estimation and evaluation of vector smooth transition autoregressive models with applications.” *CREATES Research Paper 2014-8, Aarhus University*.

Tsay R. (1998). “Testing and modeling multivariate threshold models.” *Journal of the American Statistical Association*, **93**(443), 1188–1202.

Virolainen S. (2022). “A mixture autoregressive model based on Gaussian and Student’s t -distributions.” *Studies in Nonlinear Dynamics & Econometrics*, **26**(4), 559–580.

Virolainen S. (2024). “sstvars: Toolkit for structural smooth transition vector autoregressive models.” R package version 1.0.0 available at GitHub: <https://github.com/saviviro/sstvars>.

Virolainen S. (forthcoming). “A statistically identified structural vector autoregression with endogeneously switching volatility regime.” *Journal of Business & Economic Statistics*.

Wu J., Xia F. (2016). “Measuring the macroeconomic impact of monetary policy at the zero lower bound.” *Journal of Money, Credit and Banking*, **48**(2-3), 253–291.

Appendix A Sufficient condition for stationarity and ergodicity

The sufficient condition for stationarity and ergodicity of our STVAR model, Condition 1, differs slightly from to the one in Kheifets and Saikkonen (2020, Assumption R). This is because our parametrization of the STVAR model differs from Kheifets and Saikkonen (2020). Their result is, nonetheless, applicable with our parametrization too, as is explained below.

The ergodic stationarity condition of Kheifets and Saikkonen (2020) is based on the results of Saikkonen (2008), who derived a comparable condition for smooth transition vector error correction models. Specifically, in the proof of their Theorem 1, Kheifets and Saikkonen (2020) explain how their specification can be obtained as a special from the more general nonlinear error correction model in Saikkonen (2008, Equation (17)). Our model, described in Section 2.1, is obtained as a special case from the model of Saikkonen (2008) in a similar fashion but slightly differently due to differences in the parametrization. In particular, for the first term on the right side of Saikkonen (2008), Equation (17), we consider the left side of Kheifets and Saikkonen (2020), Equation (6), with $h_s = \alpha_{m,t}$ and $\bar{B}_{sj} = A_{m,i}$. Similarly, for the third term of Saikkonen (2008), Equation (17), we consider the left side of Kheifets and Saikkonen (2020), Equation (7). Consequently, Condition 1 replaces Assumption R of Kheifets and Saikkonen (2020) as the sufficient condition for stationarity and ergodicity.

Appendix B Monte Carlo algorithm for estimating the GIRF

We present a Monte Carlo algorithm for estimating the generalized impulse response function defined in Equation (2.6) for initial values $\mathbf{y}_{t-1} = (y_{t-1}, \dots, y_{t-p})$. Our algorithm is adapted

from Koop *et al.* (1996, pp. 135-136) and Kilian and Lütkepohl (2017, pp. 601-602). We assume that the history \mathbf{y}_{t-1} follows a known distribution G , which may be such that it produces a single outcome with probability one (corresponding to a fixed \mathbf{y}_{t-1}), or it can be drawn from a specific regime as described in Section (2.2), for instance. In the following, $y_{t+h}^{(i)}(\delta_j, \mathbf{y}_{t-1})$ denotes a realization of the process at time $t + h$ conditional on the structural shock of sign and size δ_j in the j th element of e_t hitting the system at time t and on the p observations $\mathbf{y}_{t-1} = (y_{t-1}, \dots, y_{t-p})$ preceding the time t , whereas $y_{t+h}^{(i)}(\mathbf{y}_{t-1})$ denotes an alternative realization conditional on the history \mathbf{y}_{t-1} only.

The algorithm proceeds with the following steps.

0. Set the horizon H , the numbers of repetitions R_1 and R_2 , and the sign and size δ_j for the j th structural shock that is of interest.
1. Draw an initial value \mathbf{y}_{t-1} from G .
2. Draw $H + 1$ independent realizations of the structural shock e_t from the d -dimensional standard normal distribution. Then, impose the sign and size δ_j in the j th element of the first drawn structural shock e_t to obtain e_t^* . Finally, calculate the modified reduced form shock $u_t^* = B_t e_t^*$.
3. Use the modified reduced form shock u_t^* and the rest H structural shocks ε_t obtained from Step 2 to compute realizations $y_{t+h}^{(i)}(\delta_j, \mathbf{y}_{t-1})$ for $n = 0, 1, \dots, H$, iterating forward. At $h = 0$, the modified reduced form shock u_t^* calculated from the structural shock e_t^* in Step 2 is used. From $h = 1$ onwards, the $h + 1$ th structural shock e_t is used to calculate the reduced form shock $u_{t+h} = B_{t+h} e_{t+h}$.
4. Use the rest $H + 1$ the structural shocks e_t obtained from Step 2 to compute realizations $y_{t+h}^{(i)}(\mathbf{y}_{t-1})$ for $h = 0, 1, \dots, H$, so that the non-modified reduced form shock $u_t = B_t e_t$ is used to compute the time $h = 0$ realization. Otherwise proceed similarly to the previous step.

5. Calculate $y_{t+h}^{(i)}(\delta_j, \mathbf{y}_{t-1}) - y_{t+h}^{(i)}(\mathbf{y}_{t-1})$.
6. Repeat Steps 2-5 R_1 times and calculate the sample mean of $y_{t+h}^{(i)}(\delta_j, \mathbf{y}_{t-1}) - y_{t+n}^{(i)}(\mathbf{y}_{t-1})$ for $h = 0, 1, \dots, H$ to obtain an estimate of the $\text{GIRF}(h, \delta_j, \mathbf{y}_{t-1})$.
7. Repeat Steps 1-6 R_2 times to obtain estimates of $\text{GIRF}(h, \delta_j, \mathbf{y}_{t-1})$ with different starting values \mathbf{y}_{t-1} generated from the distribution G . Then, take the sample mean and sample quantiles over the estimates to obtain point estimate and confidence intervals for the GIRF with random initial value.

Notice that if a fixed initial value \mathbf{y}_{t-1} is used, Step 7 is redundant.

Appendix C Details on the empirical application

C.1 Model selection and adequacy of the selected model

The maximum likelihood (ML) estimation of the models, residual diagnostics, and estimation of the generalized impulse response functions are carried out with the R package `sstvars` (Virolainen, 2024) in which the methods introduced in this paper have been implemented. The R package `sstvars` also contains the dataset studied in the empirical application to facilitate the reproduction of our results.

We start model selection with a preliminary examination of the sample partial autocorrelation functions (PACF) of the series, which are presented in Figure C.1 for the first 24 lags. Based on the breaks in the PACFs, an autoregressive order $p = 4$ could be reasonable for parsimonious model, and an order smaller than $p = 2$ would be clearly insufficient. Therefore, we estimate two-regime GSTVAR models with $p = 1, \dots, 5$ and find that the AIC is minimized by the order $p = 4$, whereas BIC and HQIC are minimized by the order $p = 2$. The values of the information criteria are presented in Table 1 (of the paper) together with

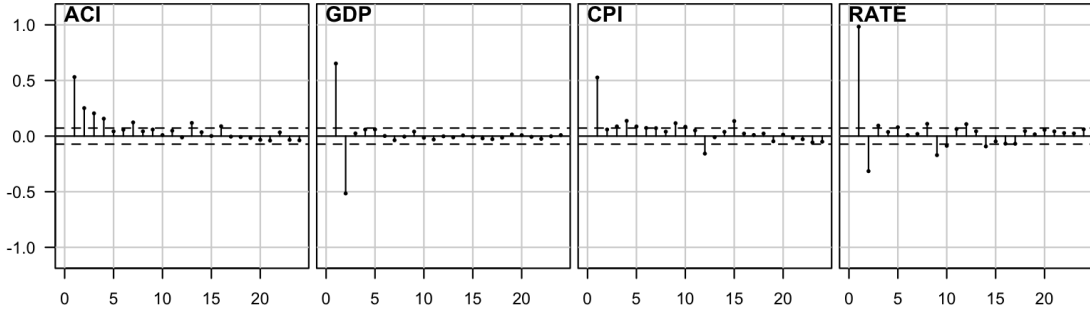


Figure C.1: Partial autocorrelation functions for the first 24 lags estimated for the monthly U.S. series covering the period from 1961I to 2022III.

the maximized log-likelihoods (divided by the number of observations).

To study whether our model adequately captures the autocorrelation structure of the data, we depict the sample autocorrelation functions (ACF) and cross-correlation functions (CCF) of the residuals for the first 24 lags in Figure C.2. As the figure shows, there is not much autocorrelation left in the residuals, but somewhat large correlation coefficient (CC) sticks out at the lag seven in the ACF of the interest rate variable. Moreover, there are somewhat large CCs at the lag zero also in the CCFs between CPI and GDP. Nevertheless, the fitted models seems to capture the autocorrelation structure of the data reasonably well.

In order to study the model's adequacy to capture the conditional heteroskedasticity of the data, we depict the sample ACFs and CCFs of squared standardized residuals for the first 24 lags in Figure C.3. The figure shows that there are several large CCs in the ACFs of the squared standardized residual of GDP and CPI. Otherwise, the CCs are not particularly large. That is, some of the conditional heteroskedasticity of GDP and CPI is not adequately captured, but in our view, the inadequacies are not very severe.

The series of standardized residuals, presented in the top panels of Figure C.4, also show some remaining heteroskedasticity and several outliers. There is a particularly large negative residual of the GDP growth rate in the beginning of the COVID-19 crisis, when the lockdown of the economy caused a substantial drop in the GDP. However, since the COVID-19 drop was caused by an exceptionally large exogenous shock, a large residual is expected for a correctly

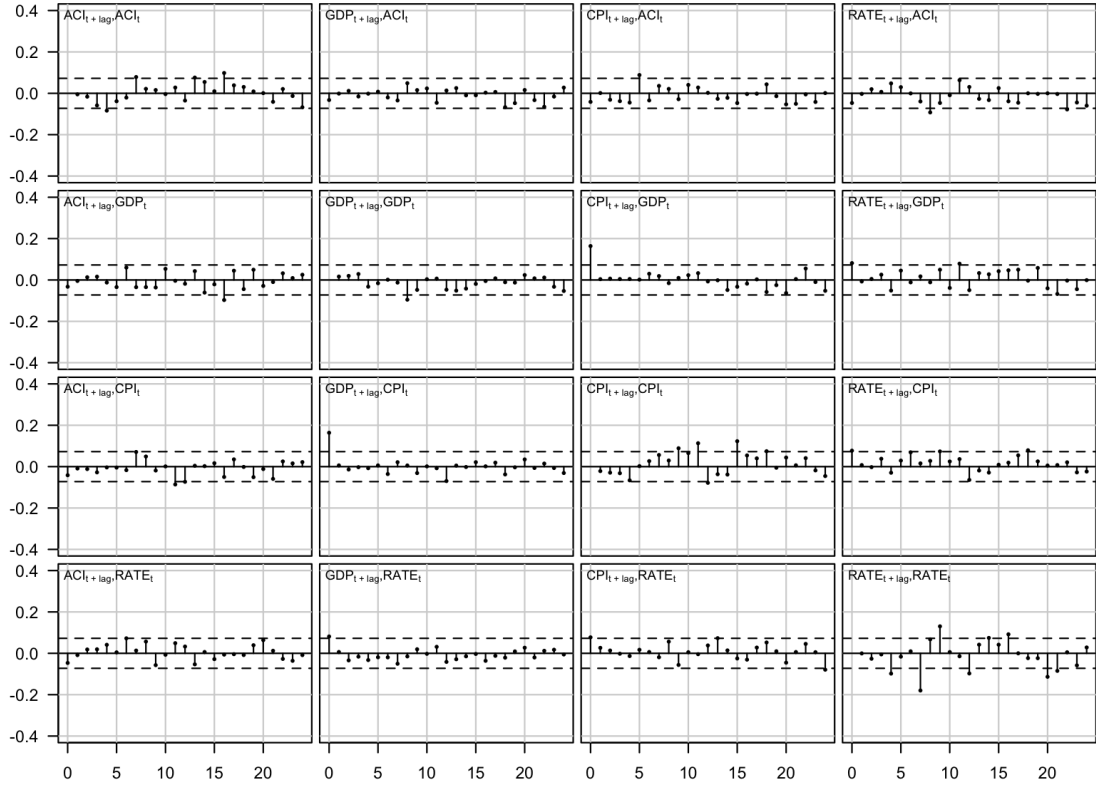


Figure C.2: Auto- and crosscorrelation functions of the residuals of the fitted two-regime GSTVAR $p = 4$ model for the lags $0, 1, \dots, 24$. The lag zero autocorrelation coefficients are omitted, as they are one by convention. The blue dashed lines are the 95% bounds $\pm 1.96/\sqrt{T}$ ($T = 731$ as the first $p = 4$ observations were used as the initial values) for autocorrelations of IID observations.

specified model. Finally, the normal quantile-quantile-plots, presented in the bottom panel of Figure 1, show that the marginal distribution of ACI is captured well. The marginal distributions of the residuals of the other variables, however, display excess kurtosis, but they are quite symmetric. Nonetheless, the overall adequacy of the model seems reasonable enough for impulse response analysis.

C.2 Robustness checks

As a robustness check, we consider the subsample period from 1963:4 to 2019:5 studied by Kim *et al.* (2022). The ACI and interest rate variable series are similar to Kim *et al.* (2022), but our data differs from them in two main aspects. First, instead of using unemployment

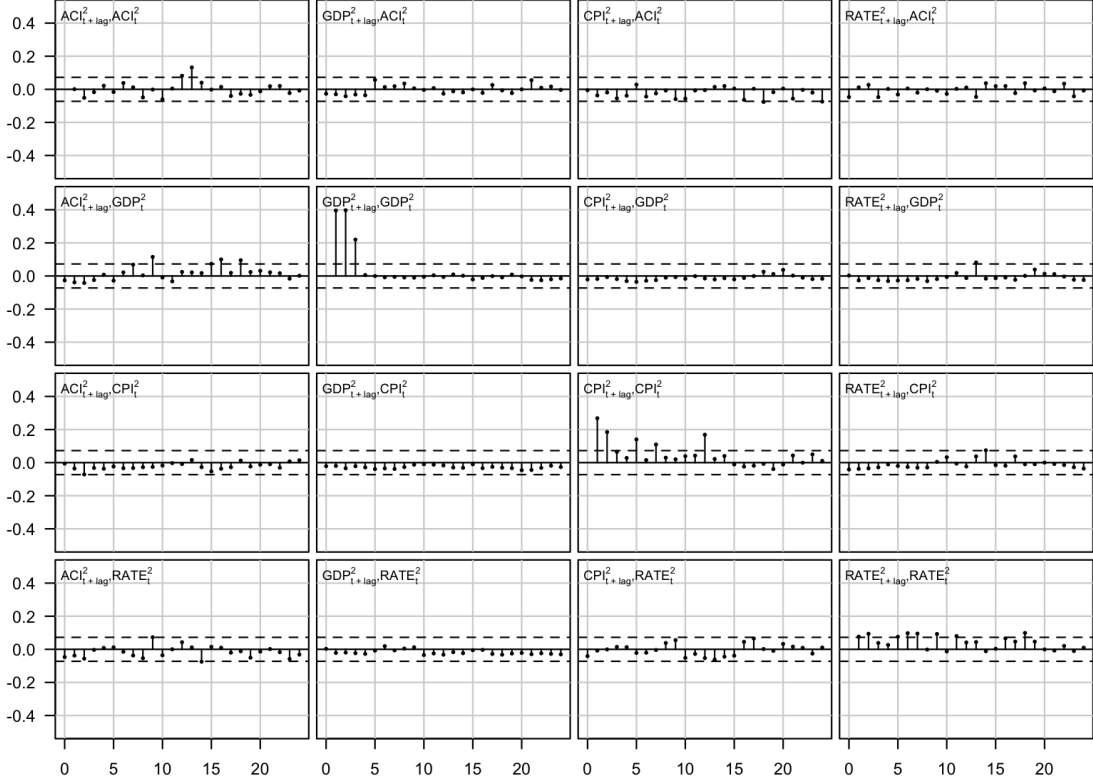


Figure C.3: Auto- and crosscorrelation functions of the squared standardized residuals of the fitted two-regime fourth-order GSTVAR model for the lags $0, 1, \dots, 24$. The lag zero autocorrelation coefficients are omitted, as they are one by convention. The blue dashed lines are the 95% bounds $\pm 1.96/\sqrt{T}$ ($T = 731$ as the first $p = 4$ observations were used as the initial values) for autocorrelations of IID observations.

rate and year-on-year industrial production index as a measure of real economic activity, we use the monthly GDP growth rate described in Section 4. Second, instead of using year-on-year CPI inflation rate, we use the monthly CPI inflation growth rate.

We fit two-regime GSTVAR models the subsample and select the autoregressive order $p = 4$ based on information criteria and preliminary examinations of partial autocorrelation functions of the series (not shown). The estimated transition weights of our two-regime fourth-order GSTVAR model are presented Figure C.5 with the shaded areas indicating the periods of NBER based on U.S. recessions. As the transition weights show, the regimes are quite similar to the benchmark specification: Regime 1 mainly dominates in the volatile period of 1960's, 1970's, and 1980's, but obtains large weights also in the 1990's recession and

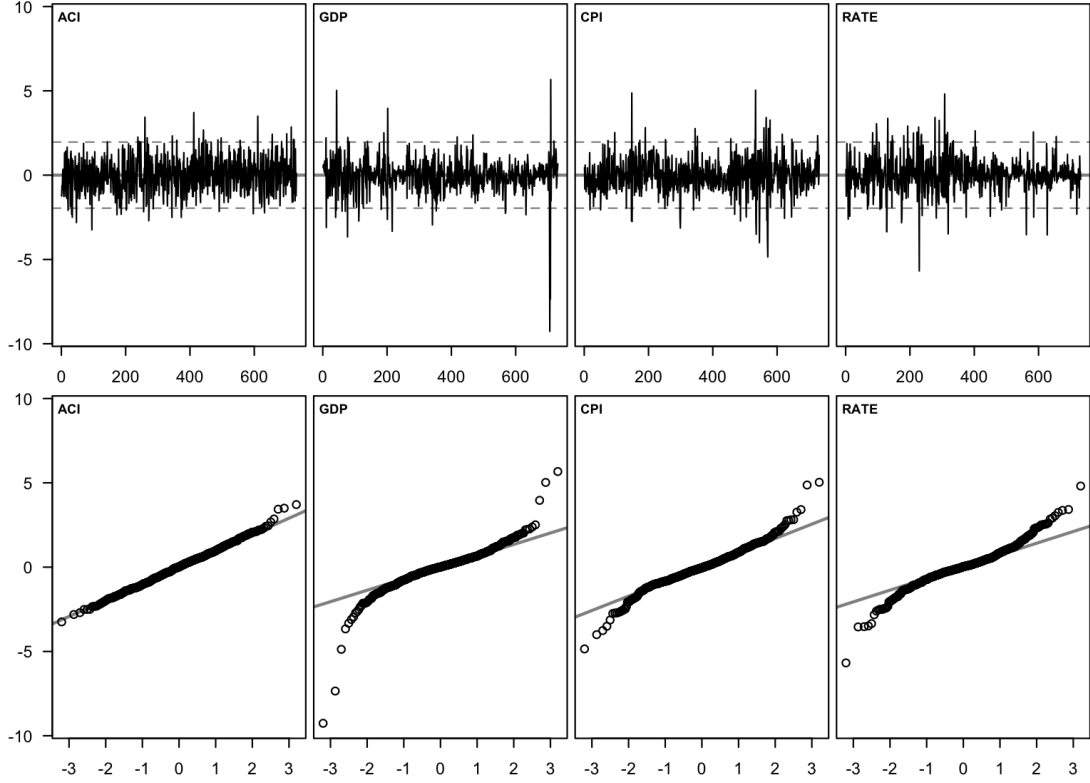


Figure C.4: Standardized residual time series and normal quantile-quantile-plots of the fitted two-regime fourth-order GSTVAR model.

the Financial crisis. Conversely, Regime 2 dominates when the first one does not.

The GIRFs estimated for the model are presented in Figure C.6, which is similar to Figure 2 of the main paper. The GIRFs are mostly similar to our main specification utilizing the full sample period from 1961:1 to 2022:3. In both of the regimes, a positive ACI shock decreases GDP and consumer prices, but the effects are stronger in Regime 1. The GIRFs are close to linear in Regime 1, and while there is variation in the GIRFs depending on the initial values in Regime 2, the effects of positive and negative shocks (as well as the effects small and large shocks not shown in Figure C.6) are very similar. A notable difference to our main specification is that a positive ACI shock increases the interest rate in Regime 1 but decreases it in Regime 2.

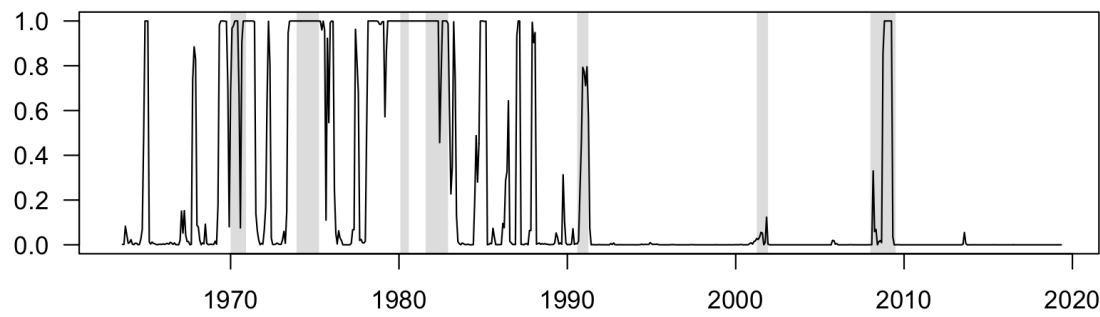


Figure C.5: Estimated transition weights of the first regime for the two-regime fourth-order GSTVAR model fitted to the monthly U.S. data covering the period from 1963:4 to 2019:5. The shaded areas indicate the period of NBER based U.S. recessions.

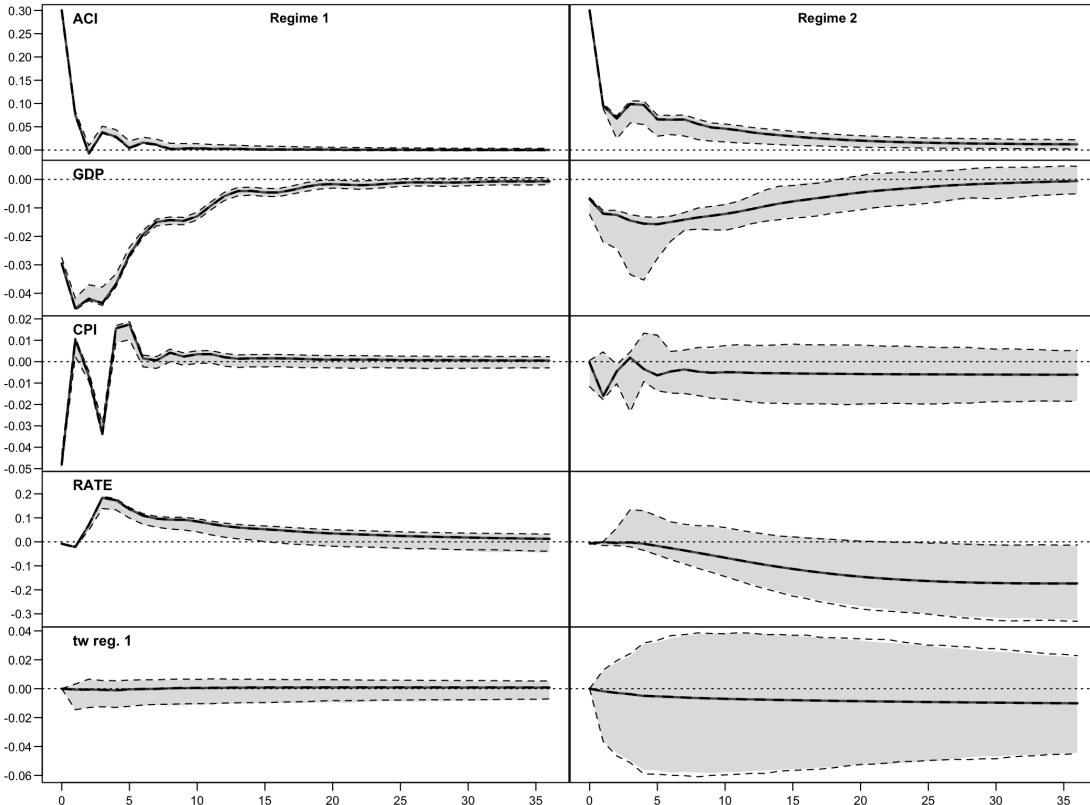


Figure C.6: Generalized impulse response functions to the identified ACI shock $h = 0, 1, \dots, 36$ months ahead, based on the data from 1963:4 to 2019:5. From the top to bottom, the responses of the ACI index, GDP growth rate, inflation growth rate, the interest rate variable, and transition weights of Regime 1 are depicted in each row, respectively. The left column shows the responses to positive (grey solid line) and negative (black dashed line) one-standard-error shocks with initial values generated from the stationary distribution of Regime 1. All GIRFs have been scaled so that instantaneous effect of the ACI index is 0.3. For a positive ACI shock, the 95% confidence intervals that reflect uncertainty about the initial state within the given regime are depicted with shaded grey areas, whereas for a negative ACI shock, they are depicted with black dashed lines. The results are based on 2500 draws of initial values (see Appendix B for details).